First publ. in: Optics Express ; 17 (2009), 15. - S. 12813-12820

Fluctuating nanomechanical system in a high finesse optical microcavity

Ivan Favero[1, 2] *, Sebastian Stapfner[1], David Hunger[1], Philipp Paulitschke[1], Jakob Reichel[3], Heribert Lorenz[1], Eva M. Weig[1], Khaled Karrai[1]

[1]*Fakultät für Physik and Center for NanoScience (CeNS), Ludwig-Maximilians-Universität, Geschwister Scholl-Platz 1, 80539 München, Germany*

[2]*Laboratoire Matériaux et Phénomènes Quantiques, Université Paris-Diderot, CNRS, UMR 7162, 10 rue Alice Domon et Léonie Duquet, 75013 Paris, France*

[3]*Laboratoire Kastler Brossel, Ecole Normale Supérieure, Université Pierre et Marie Curie, CNRS, 24 rue Lhomond, 75005 Paris, France*

** ivan.favero@univ-paris-diderot.fr*

Abstract: The idea of extending cavity quantum electrodynamics experiments to sub-wavelength sized nanomechanical systems has been recently proposed in the context of optical cavity cooling and optomechanics of deformable cavities. Here we present an experiment involving a single nanorod consisting of about 10^9 atoms precisely positioned into the confined mode of a miniature high finesse Fabry-Pérot microcavity. We show that the optical transmission of the cavity is affected not only by the static position of the nanorod but also by its vibrational fluctuation. The Brownian motion of the nanorod is resolved with a displacement sensitivity of 200 fm/$\sqrt{\text{Hz}}$ at room temperature. Besides a broad range of sensing applications, cavity-induced manipulation of optomechanical nanosystems and back-action is anticipated.

OCIS codes: (350.3950) Micro-optics, (350.4238) Nanophotonics and photonic crystals, (280.4788) Optical sensing and sensors, (140.3948) Microcavity devices, (020.5580) Quantum electrodynamics, (060.2310) Fiber optics.

References and links

1. H. Mabuchi, Q. A. Turchette, M. S. Chapman, and H. J. Kimble, "Real-time detection of individual atoms falling through a high-finesse optical cavity," Opt. Lett. **21**(17), 1393 (1996).
2. S. Haroche, and J. M. Raymond, *Exploring the Quantum* (Oxford University Press, Oxford, 2006).
3. H. J. Kimble, "Strong interactions of Single Atoms and Photons in Cavity QED," Phys. Scr. **T76**(1), 127–137 (1998).
4. I. Favero, and K. Karrai, "Cavity cooling of a nanomechanical resonator by light scattering," N. J. Phys. **10**(9), 095006 (2008).
5. V. Vuletic, and S. Chu, "Laser cooling of atoms, ions, or molecules by coherent scattering," Phys. Rev. Lett. **84**(17), 3787–3790 (2000).
6. P. Maunz, T. Puppe, I. Schuster, N. Syassen, P. W. H. Pinkse, and G. Rempe, "Cavity cooling of a single atom," Nature **428**(6978), 50–52 (2004).
7. I. Favero, and K. Karrai, "Optomechanics of deformable optical cavities," Nat. Photonics **3**(4), 201–205 (2009).
8. V. B. Braginsky, and A. B. Manukin, *Measurement of weak forces in physics experiments* (Chicago University Press, Chicago, 1977).
9. C. H. Metzger, and K. Karrai, "Cavity cooling of a microlever," Nature **432**(7020), 1002–1005 (2004).
10. O. Arcizet, P. F. Cohadon, T. Briant, M. Pinard, and A. Heidmann, "Radiation-pressure cooling and optomechanical instability of a micromirror," Nature **444**(7115), 71–74 (2006).
11. S. Gigan, H. R. Böhm, M. Paternostro, F. Blaser, G. Langer, J. B. Hertzberg, K. C. Schwab, D. Bäuerle, M. Aspelmeyer, and A. Zeilinger, "Self-cooling of a micromirror by radiation pressure," Nature **444**(7115), 67–70 (2006).
12. A. Schliesser, P. Del'Haye, N. Nooshi, K. J. Vahala, and T. J. Kippenberg, "Radiation pressure cooling of a micromechanical oscillator using dynamical backaction," Phys. Rev. Lett. **97**(24), 243905 (2006).
13. T. Corbitt, Y. Chen, E. Innerhofer, H. Müller-Ebhardt, D. Ottaway, H. Rehbein, D. Sigg, S. Whitcomb, C. Wipf, and N. Mavalvala, "An all-optical trap for a gram-scale mirror," Phys. Rev. Lett. **98**(15), 150802 (2007).
14. D. Kleckner, and D. Bouwmeester, "Sub-kelvin optical cooling of a micromechanical resonator," Nature **444**(7115), 75–78 (2006).
15. J. D. Thompson, B. M. Zwickl, A. M. Jayich, F. Marquardt, S. M. Girvin, and J. G. E. Harris, "Strong dispersive coupling of a high-finesse cavity to a micromechanical membrane," Nature **452**(7183), 72–75 (2008).

#110547 - $15.00 USD Received 27 Apr 2009; accepted 30 Jun 2009; published 13 Jul 2009

16. O. Arcizet, P.-F. Cohadon, T. Briant, M. Pinard, A. Heidmann, O. Français, and L. Rousseau, "High-sensitivity optical monitoring of a micromechanical resonator with a quantum-limited optomechanical sensor," Phys. Rev. Lett. **97**(13), 133601 (2006).
17. M. D. LaHaye, O. Buu, B. Camarota, and K. C. Schwab, "Approaching the quantum limit of a nanomechanical resonator," Science **304**(5667), 74–77 (2004).
18. F. Marquardt, J. G. E. Harris, and S. M. Girvin, "Dynamical multistability induced by radiation pressure in high-finesse micromechanical optical cavities," Phys. Rev. Lett. **96**(10), 103901 (2006).
19. D. Rugar, H. J. Mamin, and P. Guethner, "Improved fiber-optic interferometer for atomic force microscopy," Appl. Phys. Lett. **55**(25), 2588 (1989).
20. C. A. Regal, J. D. Teufel, and K. W. Lehnert, "Measuring nanomechanical motion with a microwave cavity interferometer," Nat. Phys. **4**(7), 555–560 (2008).
21. L. Sekaric, M. Zalalutdinov, S. W. Turner, A. T. Zehnder, J. M. Parpia, and H. G. Craighead, "Nanomechanical resonant structures as tunable passive modulators of light," Appl. Phys. Lett. **80**(19), 3617 (2002).
22. M. Li, W. H. P. Pernice, C. Xiong, T. Baehr-Jones, M. Hochberg, and H. X. Tang, "Harnessing optical forces in integrated photonic circuits," Nature **456**(7221), 480–484 (2008).
23. M. Wendel, H. Lorenz, and J. P. Kotthaus, "Sharpened electron beam deposited tips for high resolution atomic force microscope lithography and imaging," Appl. Phys. Lett. **67**(25), 3732 (1995) (Nanotools, Munich, Germany. www.nanotools.com).
24. M. M. J. Treacy, T. W. Ebbesen, and J. M. Gibson, "Exceptionally high Young's modulus observed for individual carbon nanotubes," Nature **381**(6584), 678–680 (1996).
25. L. D. Landau, and E. M. Lifschitz, *Mechanics* (Pergamon, New York, 1976).
26. Y. Colombe, T. Steinmetz, G. Dubois, F. Linke, D. Hunger, and J. Reichel, "Strong atom-field coupling for Bose-Einstein condensates in an optical cavity on a chip," Nature **450**(7167), 272–276 (2007).
27. N. O. Azak, M. Y. Shagam, D. M. Karabacak, K. L. Ekinci, D. H. Kim, and D. Y. Jang, "Nanomechanical displacement detection using fiber-optic interferometry," Appl. Phys. Lett. **91**(9), 093112 (2007).
28. see a similar discussion in the case of a Fabry-Pérot interferometer measuring the displacement of one of its two mirrors in V. B. Braginsky, and F. Khalili, *Quantum Measurement* p 137 (Cambridge University Press, Cambridge, 1995).
29. Y. T. Yang, C. Callegari, X. L. Feng, K. L. Ekinci, and M. L. Roukes, "Zeptogram-scale nanomechanical mass sensing," Nano Lett. **6**(4), 583–586 (2006).
30. H. G. Craighead, "Nanoelectromechanical systems," Science **290**(5496), 1532–1535 (2000).
31. I. Favero, C. Metzger, S. Camerer, D. König, H. Lorenz, J. P. Kotthaus, and K. Karrai, "Optical cooling of a micromirror of wavelength size," Appl. Phys. Lett. **90**(10), 104101 (2007).
32. I. De Vlaminck, J. Roels, D. Taillaert, D. Van Thourhout, R. Baets, L. Lagae, and G. Borghs, "Detection of nanomechanical motion by evanescent light wave coupling," Appl. Phys. Lett. **90**(23), 233116 (2007).
33. A. Ayari, P. Vincent, S. Perisanu, M. Choueib, V. Gouttenoire, M. Bechelany, D. Cornu, and S. T. Purcell, "Self-oscillations in field emission nanowire mechanical resonators: a nanometric dc-ac conversion," Nano Lett. **7**(8), 2252–2257 (2007).

1. Introduction

Confining a laser field between two high reflectivity mirrors of a high-finesse cavity can increase the probability of a given cavity photon to be scattered by an atom traversing the confined photon mode [1]. This enhanced coupling between light and atoms is successfully employed in cavity quantum electrodynamics experiments and led to a very prolific research in quantum optics [2,3]. The idea of extending such experiments to sub-wavelength sized nanomechanical systems has been recently proposed [4] in the context of optical cavity cooling [5,6] and optomechanics of deformable cavities [7]. Generally, optomechanical systems combine an optical cavity and a (typically macro- or micron-scale) mechanical oscillator in a single device, leading to an increased coupling between them [8–15]. They have recently advanced into the fields of precision displacement measurement [16], investigation of mechanical systems close to their quantum-ground state [17], non-linear dynamics [18], or sensing applications [19]. In these systems, mechanical oscillators of various sizes are now being used: from a centimetre scale movable mirror [13] down to a 100 nm-sized beam integrated in a microwave strip line [20]. At the same time, nanomechanical sytems are being optically controlled without the use of a cavity [21,22]. Here we investigate a system for cavity nano-optomechanics in the optical domain, where a 100 nm diameter vibrating nanorod is coupled to a high finesse optical micro-cavity of small mode volume.

2. Nanomechanical system

For our experiment, we choose carbon-based nanorods which combine a large mechanical stiffness, low mass and flexible device preparation. Each nanorod is grown by Electron-Beam

#110547 - $15.00 USD Received 27 Apr 2009; accepted 30 Jun 2009; published 13 Jul 2009

Deposition (EBD) [23] at the front extremity of a silicon microlever (Nanosensors PPT-CONTR: thickness = 2 μm, width = 50 μm, length = 450 μm, resonance frequency = 13 kHz) used for atomic force microscopy (AFM). As shown in Fig. 1a the nanorod extends along the lever axis, as opposed to conventional AFM cantilever probes with the tip perpendicular to the lever plane. The shape of the nanorods is slightly conical (Fig. 1b) with lengths ranging from 3 to 5 μm and mean diameters between 80 and 160 nm. First, we investigate the mechanical properties of the rods by ultrasonic actuation. To this end, the silicon lever hosting the nanorod is mounted on a high frequency piezo-transducer and placed in the chamber of a Scanning Electron Microscope (SEM) at a pressure of about 10^{-6} mbar. With a frequency generator (RS SML02), the piezo-transducer is excited to actuate the oscillator. The mechanical response of the microlever-nanorod system is simultaneously investigated by monitoring the envelope of the resulting oscillation using the SEM video images [24]. Around 13 kHz, the first flexural mode of the host silicon lever is found in compliance with its specs, with a vibration amplitude of a few tens of microns at resonance. Other modes of the microlever are observed up to 300 kHz. At higher frequency, the lowest vibrational resonance of the nanorod itself is identified at f_1 = 1.9 MHz (see inset of Fig. 1b at resonance). At a piezo excitation power of 20 μW the full width at half maximum amounts to FWHM = 300 Hz, leading to a mechanical quality factor Q = 6500 ± 2500, defined as Q = f/FWHM. When increasing the excitation power to 126 μW, the resonance develops a hysteresis upon sweeping the drive frequency up and down, revealing a non-linear dynamical behavior [25].

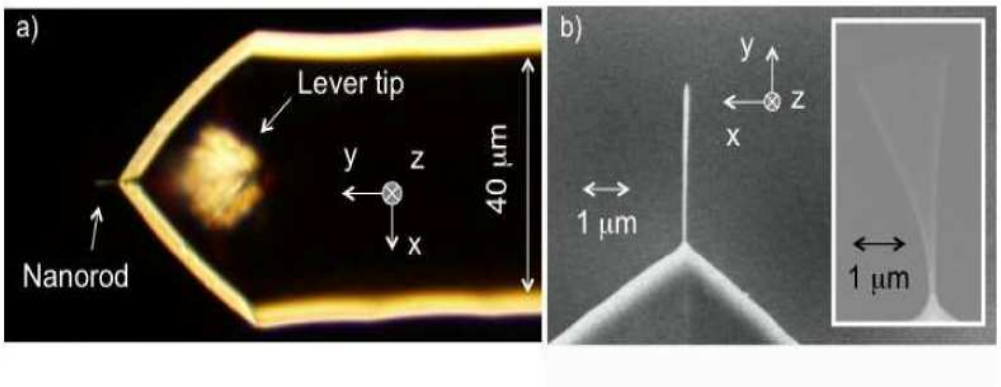

Fig. 1. Ultrasonic actuation of the nanorod flexural resonance. a) Micrograph of the AFM cantilever with a nanorod at its extremity. b) Main panel: SEM picture of an EBD nanorod grown at the end of an AFM lever. Inset: Piezo-actuated vibrational resonance of nanorod 1 flexural ground mode at 1.9 MHz imaged in the SEM.

In order to avoid excess EBD deposition during SEM inspection, which leads to a shift in resonance frequencies, and to allow characterization of the nanorod oscillators in ambient conditions, the above experiments are repeated at room pressure using a diffraction limited high magnification factor (× 500) optical microscope. The nanorods scatter light efficiently enough to make them easily visible under the microscope. Furthermore the convenience of this technique enables rapid cycling through the characterization of nanorods of successive fabrication batches and allows to determine realistic values of the quality factor at atmospheric pressure. Even though composition and material properties of EBD-grown carbon-based material are not well controlled, vibrational eigenfrequencies in the MHz range with high Q in air (10^2 to 10^3) are consistently observed on a set of 14 nanorods (see Table 1).

#110547 - $15.00 USD Received 27 Apr 2009; accepted 30 Jun 2009; published 13 Jul 2009

Table 1. Mechanical resonances of the nanorods

	Nanorod	f_1(MHz)	Q_1	f_2(MHz)	Q_2	f_3(MHz)	Q_3
Batch 1	nanorod 1	1.90 (-x)	6500 ± 2500 (vacuum)				
	nanorod 2	1.67 (-x)	170 ± 100				
	nanorod 3	1.88 (-x)	1900 ± 500				
Batch 2	nanorod 4	0.936 (-x)	460 ± 250	1.67 (-x)			
Batch 3	nanorod 5	0.363 (-x)	190 ± 90	0.601 (-x)	260 ± 100	1.172 (-z)	250 ± 100
	nanorod 6	0.474 (-z)	250 ± 100	0.784 (-z)	250 ± 150		
Batch 4	nanorod 7	1.706 (-z)	630 ± 300	4.375 (-z)	1200 ± 450		
	nanorod 8	1.072 (-z)	390 ± 150	1.497 (-z)	340 ± 200		
	nanorod 9	1.162 (-z)	360 ± 200				
	nanorod 10	1.138 (-z)	570 ± 250				
	nanorod 11	1.300 (-z)	500 ± 200				
Batch 5	nanorod 12	1.059 (-z)	415 ± 100	1.479 (-z)	525 ± 150	1.677 (-x)	930 ± 300
	nanorod 13	0.981 (-z)	630 ± 250	1.371 (-z)	480 ± 250		
	nanorod 14	1.691 (-z)	420 ± 200				

Mechanical resonances of the nanorods characterized at atmospheric pressure and room temperature by ultrasonic actuation using optical microscope imaging. Nanorod 1 was investigated under vacuum in the SEM. (-x) and (-z) indicate the direction of the nanorod vibration (see Fig. 1). Frequencies f_1, f_2 and f_3 are the three lowest vibrational frequencies identified when performing the experiment. Q_1, Q_2 and Q_3 denote the respective quality factors.

3. Positioning the nanorod in the microcavity

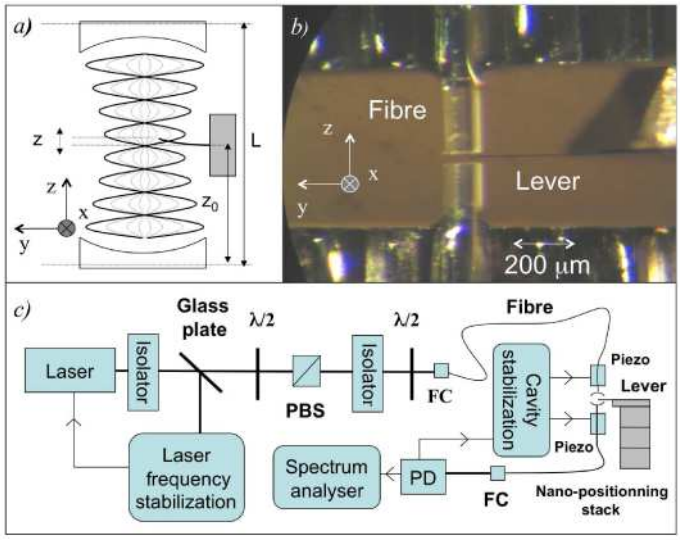

Fig. 2. Nanorod vibrating in the microcavity resonantly probed by a laser. a) Schematics of nanorod at position z_0 in the microcavity and vibrating with an amplitude z. b) Optical micrograph of the host silicon lever plunged between the two fibre end-facets in order to position the nanorod in the cavity mode. c) Set-up schematics (PBS: polarizing beam splitter, FC: fibre coupler, PD: photodiode).

Following the mechanical characterization, the nanorod is positioned into the optical microcavity as depicted schematically in Fig. 2a. The micron-sized Fabry-Pérot cavity, optimized for a wavelength of 780 nm, consists of two Bragg-coated concave fibre end-facets formed by CO2 laser machining [26]. It has a stable cavity mode of waist radius 3.4 µm and a

#110547 - $15.00 USD Received 27 Apr 2009; accepted 30 Jun 2009; published 13 Jul 2009

measured finesse of F = 5000. An external cavity laser diode is frequency-stabilized on a Rubidium atomic resonance and coupled into the input fibre (Fig. 2c), while collecting the cavity transmission and reflection on pre-amplified photodiodes. A half wave-plate placed before the input fibre is used to select one of the two linearly polarized ground modes of the cavity. The experiment is performed at ambient pressure and room temperature. To manipulate the nanorod in the cavity, the host silicon lever along with the piezo-actuator is glued on a thin copper holder and mounted in turn on a XYZ nano-positioning stack (Attocube ANP100), allowing precise positioning of the nanorod over a range of 5 mm in all three directions. The 2 μm thin silicon lever allows inserting the nanorod into the 42 μm gap between the two micromirrors, thus entering the optical mode region (see Fig. 2b). The optical set-up schematics are shown in Fig. 2c.

The position of the nanorod along the mode modifies the cavity transmission. For each position (x,y) of the nanorod in the plane transverse to the optical axis Z for a given z_0, the resonant transmission T(x,y) is measured. The 2D plot of T(x,y) is shown in Fig. 3a. Fig. 3b, for comparison, displays a simulation of T(x,y) using the expression derived in ref [4] $T(x,y) = 1/(1 + (4F/\pi)\Sigma_1(x,y)\sin^2(kz_0))^2$ in the limit of $\Sigma_1 << g$ and $z_0 \neq 0$. The scattering parameter $\Sigma_1(x,y)$ (see [4]) is assumed to be proportional to the convolution of the cavity mode cross-section (Fig. 3c) with the cross-section of the nanorod attached to the end of the microlever (Fig. 3d). The comparison between Figs. 3a and 3b allows to determine the optimum (x,y) position of the nanorod in the cavity for subsequent measurements: this position is chosen in order for the nanorod to perturb the cavity mode, while making sure the silicon lever does not contribute much to the perturbation. To this end, we focus on situations where the nanorod is positioned to reduce the resonant transmission by a factor of 2 (see e.g. arrow in Figs. 3a and 3b, corresponding to the situation shown in Fig. 3e).

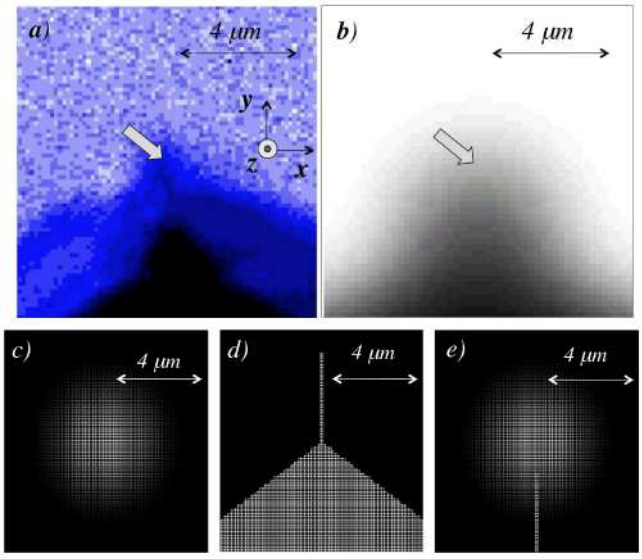

Fig. 3. In situ positioning of the nanorod in the cavity mode. a) Imaging of the nanorod in the cavity mode trough the cavity transmission T(x,y). The arrow indicates the operating point where the resonant transmission is reduced by a factor 2. b) Simulated cavity transmission T(x,y) (the pixels show the grid taken for computation). Arrow at the same position as in a). c) Cross-section of a Gaussian mode intensity distribution representing the cavity mode. d) Planar section of the nanorod placed at the end of the AFM lever. e) Nanorod position in the cavity mode, corresponding to the arrow in a) and b).

4. Optical cavity read-out of nanomechanical motion

Positioning the nanorod according to Fig. 3e allows to image the standing wave intensity distribution in the resonant cavity by moving the nanorod base position z_0 along Z while

#110547 - $15.00 USD Received 27 Apr 2009; accepted 30 Jun 2009; published 13 Jul 2009

keeping the x- and y-coordinate fixed (see Fig. 2a) and simultaneously recording the cavity transmission and reflection. The resulting graph is shown in Fig. 4a. It has the expected λ/2 periodicity. To read out the position fluctuations of the nanorod in the noise spectrum of the transmission with the highest sensitivity, we select a position z_0 of maximal gradient dT/dz_0 (arrow in Fig. 4a) and lock the cavity on resonance with the laser. Data obtained with nanorod 6 (see Table 1) are shown in Figs. 4b and 4c. Fig. 4b displays a clear resonance around 13 kHz that is observed 20 dB above the noise floor and which reflects the thermal motion of the host silicon lever. Indeed, the lever vibrational motion translates to a motion of the nanorod base position z_0 of small amplitude << λ/2, which modulates the cavity transmission in proportion to dT/dz_0. Using the value of dT/dz_0, the amplitude of the z_0 motion can be inferred from the transmission noise spectrum (see Fig. 4b). An excellent fit is obtained using a harmonic oscillator model for the lever flexural thermal motion, which is described by the amplitude component $z_{0,\omega}$ at angular frequency $\omega = 2\pi f$ in a frequency window δf

$$\frac{\left|z_{0,\omega}\right|^2}{\delta f} = \frac{k_B T}{K} \frac{\Gamma \omega_0^2}{\left(\omega_0^2 - \omega^2\right)^2 + (\omega\Gamma)^2} \qquad (1)$$

where K is the lever spring constant, f_0 its eigenfrequency and Γ its damping rate, such that $Q = (2\pi/\sqrt{3})(f_0/\Gamma)$. From the fit, we obtain K = 0.21 N/m and f_0 = 13.17 kHz, in agreement with the specifications of the lever, and Q = 14, a typical value for an AFM lever at room pressure. At higher frequencies, we observe three resonances: at f_1 = 473 kHz (Fig. 4c, 5 dB above the noise floor), at f_2 = 784 kHz (Fig. 4c inset, 3 dB above the noise floor) and a third at f_3 = 1.172 MHz, which appears as a slight protrusion over the noise floor. They are the three eigenmodes of nanorod 6 already identified by piezo-actuation under the optical microscope (see Table 1). For calibration purposes, the experiment is repeated in the cavity under external piezo-actuation of the nanorod at the same position z_0 (arrow in Fig. 4a). We measure the response of the cavity transmission to this externally driven vibrational excitation in the low amplitude limit (z<< λ/2). Under our experimental conditions, the cavity transmission responds linearly in dT/dz_0 and in z. This calibration allows deducing the nanorod first flexural mode vibrational amplitude z (shown in Fig. 4c) from the noise measurement when the external driving is switched off. However, because of the limited resolution of the optical microscope, we estimated this calibration to be valid only within a factor 3. Using the harmonic oscillator model from Eq. (1), we fitted the resonance spectrum of the first thermally driven mode of nanorod 6 and obtained f_1 = 473.4 kHz, K_{rod} = 1.35 N/m and Q_1 = 215, in perfect agreement with the piezo-actuation experiments.

The data in Fig. 4c yield a detection sensitivity of 200 fm/√Hz, which is on par with values previously obtained for room temperature detection of nanoresonator displacement (e.g. 300 fm/√Hz in [27]). The demonstrated sensitivity is so far limited here by the spectrum analyzer noise level. The shot-noise of light crossing the cavity sets a lower bound to the amplitude of the vibrational fluctuation which can be read-out in the transmission. This bound is $(1/(dP_t/dz)) \times (2h\nu P_t)^{1/2}$ where P_t is the transmitted optical power and hν the energy of an incident photon [28]. In the present experiment, this amounts to 100 fm/√Hz, very close to our observed sensitivity.

#110547 - $15.00 USD Received 27 Apr 2009; accepted 30 Jun 2009; published 13 Jul 2009

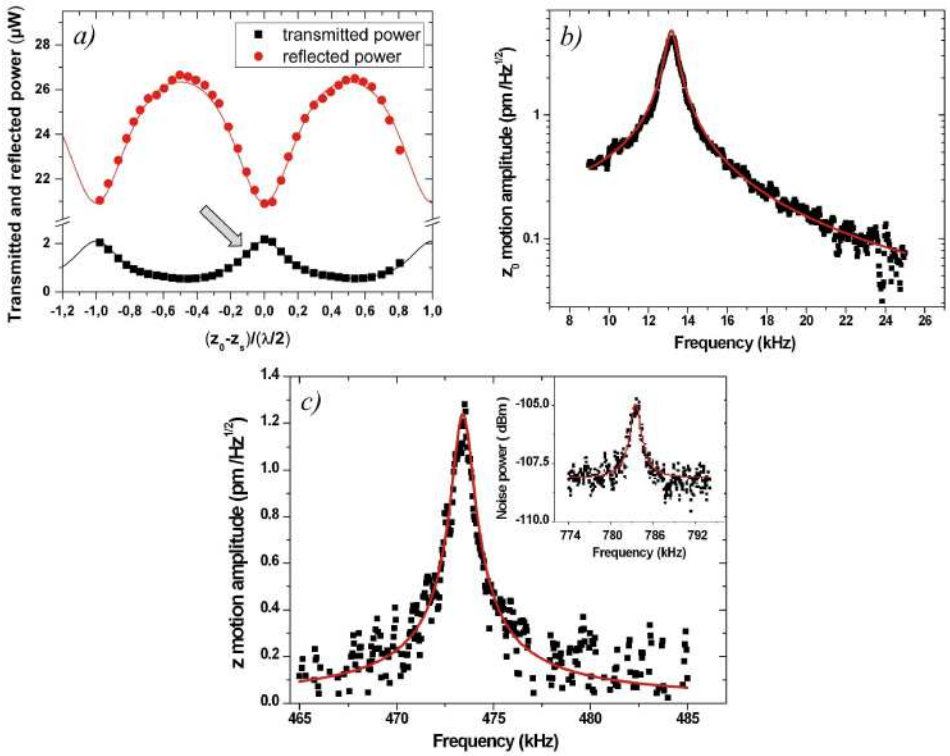

Fig. 4. Perturbation of the cavity transmission by the nanorod. a) Optical power transmitted and reflected by the cavity at resonance as a function of the nanorod base position z_0 normalized to the laser wavelength λ (z_s being the average position of the lever, roughly in the middle of the cavity). The arrow indicates the operating point of maximum gradient dT/dz_0. b) Brownian motion amplitude spectrum and fit of the AFM lever extremity z_0 holding the nanorod, from noise measurement taken at maximum gradient dT/dz_0. c) Brownian motion amplitude spectrum z for the first flexural resonance of nanorod 6. Inset: Transmission noise power spectrum around the frequency of the second flexural resonance of nanorod 6, for a resolution bandwidth of 300 Hz of the spectrum analyser.

This sensitivity can be further improved using a lower noise analyzer, a homodyne detection scheme and most importantly a better cavity. A similar fibre based microcavity of finesse 40 000 has already been demonstrated [26], which corresponds to an improvement of about one order of magnitude in comparison to the cavity used in this work. Increased finesse results in an increased value of dP_t/dx (see [4]). Additionnally, we expect in a near future to increase the transmission by 100-fold in an improved version of our apparatus. This technical improvement is definitely suggested from test cavities with optimally tuned alignment. All these improvements should bring the shot-noise limited sensitivity down to the fm/√Hz level for the same nanorod and incident power, which is close to state of the art nanomechanical displacement sensitivity reported using a single electron transistor at mK temperature [17]. Eventually the detection sensitivity will depend on the strength of the light-nanoresonator interaction. For example, when bringing in a carbon nanotube, a resonant dipole interaction of the cavity field with an excitonic line of the tube could be advantageously explored.

5. Perspectives

Such high sensitivity would allow the vibrational spectroscopy by optical means of nanomechanical resonators of virtually any size or composition. It is also an asset for detecting their mechanical response to weak perturbations in sensing applications, like ultra-sensitive mass sensing [29,30]. Used as a nanosensor, the nano-optomechanical system under investigation could benefit both from high sensitivity to inertial mass accretion, thanks to

#110547 - $15.00 USD Received 27 Apr 2009; accepted 30 Jun 2009; published 13 Jul 2009

small mass of the nanorod and its high Q in air (10^2 to 10^3), and from low-noise optical interferometry detection [27,31,32]. Even more, an improvement of the cavity finesse or a reduction of nanomechanical resonator mass would also place the system in a regime of strong optomechanical back-action [7,8]. With a single wall carbon nanotube positioned in the cavity presented here, we should observe optical self-cooling of the nanotube as well as its optically pumped self-oscillation [4,33]. Such optomechanical control combined with high optical sensitivity will eventually allow operating such nano-optomechanical sensors approaching the limit of Heisenberg fluctuations.

Acknowledgements

We gratefully acknowledge financial support of the Alexander von Humboldt Foundation, the German-Israeli Foundation (G.I.F.), the German Excellence Initiative via the Nanosystems Initiative Munich (NIM) and the Center for NanoScience.

#110547 - $15.00 USD Received 27 Apr 2009; accepted 30 Jun 2009; published 13 Jul 2009